HHS Public Access

Author manuscript

Mater Sci Eng C Mater Biol Appl. Author manuscript; available in PMC 2022 January 01.

Published in final edited form as:

Mater Sci Eng C Mater Biol Appl. 2021 January ; 120: 111693. doi:10.1016/j.msec.2020.111693.

SILVER-DOPED BIOACTIVE GLASS PARTICLES FOR *in vivo* BONE TISSUE REGENERATION AND ENHANCED METHICILLIN-RESISTANT *STAPHILOCOCCUS AUREUS* (MRSA) INHIBITION

Natalia Pajares[a], **Yadav Wagley**[b], **Chima V. Maduka**[b,c,d], **Daniel W. Youngstrom**[b], **Alyssa Yeger**[b], **Stephen F. Badylak**[e], **Neal D. Hammer**[f], **Kurt Hankenson**[b], **Xanthippi Chatzistavrou**[a,*]

[a]Department of Chemical Engineering and Materials Science, College of Engineering, Michigan State University, East Lansing, MI 48824, USA.

[b]Department of Orthopaedic Surgery, University of Michigan Medical School, Ann Arbor, MI 48103, USA

[c]Institute for Quantitative Health Sciences and Technology, Michigan State University, East Lansing, MI 48824, USA.

[d]Comparative Medicine and Integrative Biology, College of Veterinary Medicine, Michigan State University, East Lansing, MI 48824, USA.

[e]McGowan Institute for Regenerative Medicine, University of Pittsburgh, Pittsburgh, PA, USA

[f]Department of Microbiology and Molecular Genetics, Michigan State University, East Lansing, MI 48824, USA.

Abstract

[*] corresponding author: Dr. Xanthippi Chatzistavrou, Department of Chemical Engineering and Material Science, Engineering Building, 428 S. Shaw Lane, East Lansing, MI 48824, USA chatzist@msu.edu.

6. Author contribution

Natalia Pajares-Chamorro: Conceptualization, Methodology, Validation, Formal analysis, Investigation, Data curation, Writing-original draft. **Yadav Wagley**: Methodology, Validation, Investigation, Data curation. **Chima Maduka**: Formal analysis, Investigation. **Daniel Younstrom**: Investigation, Data curation. **Alyssa Yeger**: Formal analysis. **Stephen Badylak**: Resources, Writing- review & editing. **Neal Hammer:** Resources, Writing- review & editing, Funding Acquisition. **Kurt Hankenson**: Validation, Investigation, Resources, Writing- review & editing, Funding Acquisition. **Xanthippi Chatzistavrou**: Conceptualization, Resources, Writing-review & editing, Supervision, Project Administration. Funding Acquisition.

Author Statement

This manuscript has been improved after addressing the useful comments and the suggestions of the reviewers.

We believe that this work is going to be of a particular interest for the readers of the Materials Science and Engineering C journal, as it covers the challenges to deliver bioactive and antibacterial particles that can trigger bone regeneration, while additionally they present advanced synergistic antibacterial properties when they combined with antibiotics. It can be the foundation for introducing effectively new multifunctional formulations towards translational applications in the biomedical field.

7. Competing interest

The authors declare no conflict of interest in this work.

Declaration of interests

The authors declare that they have no known competing financial interests or personal relationships that could have appeared to influence the work reported in this paper.

Infection is a significant risk factor for failed healing of bone and other tissues. We have developed a sol-gel (solution-gelation) derived bioactive glass doped with silver ions (Ag-BG), tailored to provide non-cytotoxic antibacterial activity while significantly enhancing osteoblast-lineage cell growth *in vitro* and bone regeneration *in vivo*. Our objective was to engineer a biomaterial that combats bacterial infection while maintaining the capability to promote bone growth. We observed that Ag-BG inhibits bacterial growth and potentiates the efficacy of conventional antibiotic treatment. Ag-BG microparticles enhance cell proliferation and osteogenic differentiation in human bone marrow stromal cells (hBMSC) *in vitro*. Moreover, *in vivo* tests using a calvarial defect model in mice demonstrated that Ag-BG microparticles induce bone regeneration. This novel system with dual biological and advanced antibacterial properties is a promising therapeutic for combating resistant bacteria while triggering new bone formation.

Graphical Abstract

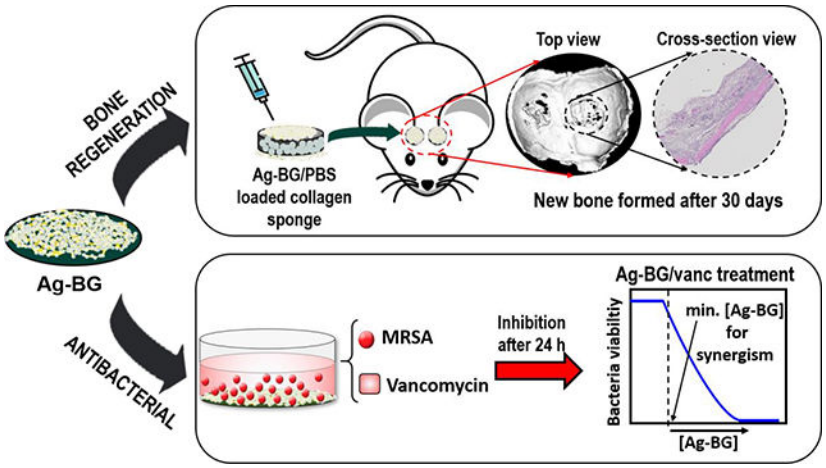

Keywords

silver doped bioactive glass; synergistic antibacterial properties; methicillin-resistant *Staphyloccocus aureus*; cell viability; cell differentiation; calvarial bone growth

1. Introduction

Antibiotic resistance is a significant public health concern. The evolution of resistant strains has become a significant challenge to combat infections caused by bacterial pathogens that were previously treatable using antibiotic therapy. Antibiotic resistance represents an enormous economic burden to the health care system with an estimated cost of 20 billion dollars per year in the United States alone [1–3]. Among the multi-resistant strains listed by the World Health Organization (WHO), *Staphylococcus aureus* (*S. aureus*) is one of the highest prioritized [4] due to the prevalence of recalcitrant isolates and the fact that this pathogen is capable of colonizing a dynamic range of host tissues. In keeping with these facts, *S. aureus* is the leading cause of skin and soft tissue infections as well as invasive tissue diseases such as endocarditis and osteomyelitis [5–8]. *S. aureus* bone infection hinders the penetration of antimicrobials by triggering pathological changes into the tissue [9].

Additionally, *S. aureus* infection [10] causes failure of almost 35% of the prosthetic joints [11]. Together these facts underscore the need for novel therapeutic strategies. In the context of bone fractures, an ideal therapy combines effective tissue engineering with sustained bactericidal activity to prevent bone infections, mitigating the risk for the development of antibiotic resistance while concurrently promoting bone regeneration.

The use of heavy metal ions (e.g. silver, copper, zinc) against drug-resistant bacteria is a promising approach for efficacious treatment and has demonstrated to be potent antibacterial agents [12–18]. The release of heavy metal ions in the body, however, raises a general toxicity concern that prevents systematic use. It is well known that silver ions (Ag^+) act as broad-spectrum biocides against different Gram-negative and Gram-positive bacteria including resistant strains. Over the past decades, research has been performed to understand various mechanisms by which Ag^+ causes bacteria death [12,18]. Due to this effect on bacteria, concerns about cytotoxic behavior frequently arise, and release in the human body raises a general toxicity concern that prevents systematic use [19]. This potential mammalian cytoxicity has resulted in the development of Ag^+-antibiotic combination treatment, which optimizes the amount of each agent required to treat the infection while minimizing the associated risks to host tissues. Research has found that both agents act synergistically, enhancing the inhibition, and expanding the spectrum of action of the antibiotics [20,21]. However, beyond the considerable antibacterial action, a material that also hosts tissue regenerative properties is still lacking. Biomaterials that treat infections and induce tissue regeneration are a promising approach to address this problem.

Bioactive glasses (BGs) have been shown to promote tissue regeneration [22,23] and have been previously modified by heavy metal ions to combat bacterial infections [24–26]. BGs have a unique set of properties, such as the ability to interact with the biological environment triggering the dynamic modification of their surface where a new highly reactive carbonated hydroxyapatite (HCA) layer forms. This HCA bonds firmly to hard and soft tissues at the interface [22,23,27]. Additionally, BGs degrade at a controllable rate releasing therapeutical ions to promote osteogenesis and angiogenesis [28]. Previous research has shown the capability of these released ions to exert gene expression of osteoblast, leading to the bone regenerative ability of this material [29,30]. This regenerative potential of BGs has been studied before in animal models from mice to sheep, mostly as 3D scaffolds since their morphology supports and sustains bone growth through the interconnected pores [31–33] and particles [34]. Different BG compositions have been developed over the years, doping the structure with a variety of ions to improve the bone-seeking properties (i.e Zn, Sr) with promising results in osseointegration [35] and other molecular and cellular pathways [36]. However, despite their positive *in vitro* results, BGs doped with heavy metals (i.e Ag, Au) [37,38], interesting for their antimicrobial capacity, have not been extensively studied *in vivo* [39][40], due to the cytotoxicity concern related to the concentration of Ag^+ leached during treatment. This research provides evidence of bone regrowth after treatment with Ag-doped BG microparticles in an animal model.

This work addresses the challenge of heavy metals toxicity by controlling the release of antimicrobial Ag^+ ions [41–45]. We used a solution-gelation (sol-gel) derived bioactive glass in powder form in the SiO_2 58.6-CaO 24.9-P_2O_5 7.2-Al_2O_3 4.2- Na_2O 1.5- K_2O 1.5- Ag_2O

2.1 wt% system that has been previously studied [46,47]. The developed Ag-BG demonstrates long-term antibacterial properties while maintaining its bioactive behavior required for tissue regeneration, as observed in previous dental applications [45–47], while for the first time this work presents *in vivo* bone regeneration.

Silicate based bioactive glasses have also been previously used as a drug delivery vehicle [48–51]. This work aims to combat resistant bacteria through an advanced synergism between the Ag-BG particles and a co-delivered antibiotic. This combination restores the sensitivity of the antibiotic presenting advanced antibacterial activity as a function of concentration and time. Additionally, the concomitant release of the ions from the bioactive and degradable glass stimulates tissue regeneration during the healing process, as mentioned before.

In the present work, the antibacterial properties of Ag-BG are studied against methicillin-resistant *Staphyloccocus aureus* (MRSA), the most common etiological agent of bone infections. Further, the cell-material interaction of Ag-BG in culture with human bone marrow stromal cells (hBMSC) was studied *in vitro*. Bone regenerative properties of these microparticles were assessed *in vivo* using a calvarial defect mouse model. Combination of Ag-BG with antibiotics against methicillin-resistant *S. aureus* (MRSA), demonstrated synergy between the glass and the antibiotic that was dependent on the concentration of both compounds. In this research, the antibiotic that was selected for co-delivery was vancomycin, which is one of the few treatments used as a last resort to treat MRSA infections. However, in low growth or growth-arrested conditions that can occur during the development of a biofilm, MRSA resists vancomycin. In addition to the antibacterial properties, Ag-BG enhanced hBMSC cell viability and differentiation. Increased bone regeneration was also observed *in vivo* in the calvarial bone model. This research supports the potential use of Ag-BG microparticles as advanced therapeutics against MRSA, while also promoting bone regeneration.

2. Methods

2.1. Synthesis of Ag-doped bioactive glass (Ag-BG)

The fabrication of Ag-BG (SiO_2 58.6-CaO 24.9-P_2O_5 7.2-Al_2O_3 4.2- Na_2O 1.5- K_2O 1.5-Ag_2O 2.1 wt%.) microparticles consisted of sol-gel acid catalysis as reported elsewhere [46]. Two systems being in their solution stage (the 58S sol-gel BG in SiO_2 58–CaO 33–P_2O_5 9 wt.% system with the respective solution stage of the sol-gel porcelain A in SiO_2 60–CaO 6–P_2O_5 3–Al_2O_3 14–Na_2O 7–K_2O 10 wt.% system) were mixed as presented in detail previously [52,53]. After stirring, the final solution was aged at 60°C, dried at 180°C and stabilized up to 700°C. The particles obtained were dry ball-milled to a fine powder and sieved to a particle size below 20 μm. Microparticles have a homogeneous distribution of elements and a glass-ceramic structure, favoring the sustained release of therapeutic ions (i.e Si, Ca, P and Ag). It was observed the sustained release of Ag^+ ions for almost up to a month, which is constantly higher than the minimum required for bactericidal properties and constantly non-toxic to eukaryotic cells [45]. The immersion of particles in buffer showed no significant change in the pH values that remained constantly neutral (~ 7.5) and yielded to a total weight loss of 3% for a month, demonstrating a non-toxic degradation of the

material [45]. The promising results obtained in dental applications support the use of these particles for orthopedic applications.

2.2. Antibacterial activity

The bactericidal properties of Ag-BG alone, vancomycin alone (vanc), and the combination of Ag-BG with vancomycin (Ag-BG/vanc) were studied against laboratory-derived methicillin-resistant *S. aureus* (MRSA) USA300 JE2 [54]. The bacterial cells were prepared by inoculating a single colony of JE2 in tryptic soy broth (TSB) overnight at 37 °C [54]. A bacterial suspension was prepared by adjusting the concentration of the overnight culture to 10^8 colony forming units (CFU)/mL in Phosphate Buffered Saline (PBS). Then, the bacterial suspension was mixed 1:1 with the corresponding treatment (Ag-BG, Ag-BG/vanc, or vanc) to a final volume of 1 mL. An untreated control was prepared by suspending bacteria 1:1 volume ratio in PBS. After 24 h of incubation at 37 °C, the results were obtained by drawing a sample of 100 μL from the 1 mL mixture suspension, following serial dilutions. Each dilution was plated in tryptic soy agar for CFU enumeration, and calculations were performed to extrapolate the result to (CFU)/mL to obtain the bacterial concentrations expected in the 1 mL suspensions after treatment. The effect of the treatments was evaluated based on the decrease of CFU compared to the negative control. Quantification of CFU was performed in biological and technical triplicates.

Previous research using the same experimental conditions determined the minimum inhibitory concentration (MIC) and minimum bacterial concentration (MBC) of Ag-BG in PBS against MRSA to be 2.5 mg/mL and 6.25 mg/mL, respectively [55]. Vancomycin (molecular formula: $C_{66}H_{75}Cl_2N_9O_{24}$•HCl, Vancomycin hydrochloride) is a cell-wall targeting antibiotic that is bactericidal against actively dividing cells and has no effect against MRSA under growth-arrested conditions. Vancomycin was selected for this work due to its previously reported synergy with Ag-BG [55]. Here, the concentration dependency of this synergy was evaluated by exposing MRSA to different combinations of Ag-BG/vanc. Two experimental set-ups were performed. Initially, 0.5 mg/mL of vancomycin were delivered together with 1.25, 2.5, 3.75 or 6.5 mg/mL of Ag-BG and then, 2.5 mg/mL of Ag-BG were combined with 0.1, 0.3, 0.5 and 1 mg/mL of vancomycin. Ag-BG powder was sterilized using UV radiation before exposure to bacteria. The antibiotic treatment was prepared by dilution of vancomycin powder at different concentrations in PBS, and the Ag-BG/vanc samples were prepared by mixing Ag-BG powder with the corresponding vancomycin solution. Note that in this experimental set-up vancomycin was not loaded but delivered together with the microparticles. Ag-BG particles are not considered as a delivery vehicle for the antibiotic.

2.3. *Proliferation and differentiation of human bone marrow stromal cells (*hBMSC*)*

Primary bone-marrow-derived human marrow stromal cells (hBMSC) were obtained from the Institute of Regenerative Medicine, Texas A&M University. Frozen vials of cells were thawed and cultured at a density of 3000 cells/cm^2 in α-MEM supplemented with 16% fetal bovine serum, 1% Antibiotic-Antimycotic (Gibco 15240062), and 1% L-glutamine (hereafter, growth medium) in a humidified 37 °C/5% CO_2 incubator. Cells were expanded until 90 % confluence to a final passage 4. At the time of seeding, cells were enzymatically

lifted from culture dishes using trypsin and then, centrifuged for 5 min. The pellet was resuspended in fresh media and cells were plated at a density of 3.0×10^4 cells/mL on each well of the 24-well plate by pipetting 0.5 mL/well. Seeding was allowed for 24 h. The Ag-BG microparticles were preconditioned for 4 days using α-MEM, centrifuged, and dried at 60 °C. The powders were sterilized using UV radiation and introduced in inserted porous transwells on the culture plates containing the hBMSC. The effect of Ag-BG in cell proliferation and differentiation was evaluated for different concentrations of Ag-BG and it was compared to a negative control consisting of cells immersed only in culture medium (hereafter, untreated cells). The media was fully refreshed every other day.

2.3.1. Cell proliferation—Cell metabolic activity and consequently, cell viability and proliferation were assessed after 2, 4, and 6 days of culture in growth medium using the MTT assay kit (Sigma Aldrich). Cells were exposed to 2.5, 5, 7.5, and 12.5 mg of Ag-BG powder. At the end of each time point, 500 μL of MTT solution was added to each well and incubated for 4 h at 37 °C to allow its cleavages to formazan by enzymes from viable cells. Then, 500 μL of the solubilization solution was added and incubated for 24 h at 37 °C to dissolve the crystals staining the culture solution. The amount of formazan dye formed allowed a correlation to the concentration of metabolically active cells in the untreated vs Ag-BG treated culture. The blue dye was measured using a spectrometer at 570 nm and the results were recorded as optical density values (OD). A schematic illustration of the experimental design is presented in Figure S1.

2.3.2. Cell differentiation—Cell differentiation to osteoblasts was evaluated in terms of gene expression and cell mineralization after exposure to 5, 7.5, and 12.5 mg of Ag-BG for 10 days (Figure S2). The expression of specific genes, including the osteoblastic genes, bone sialoprotein (BSP), and osteocalcin (OCN), was evaluated using RT-PCR. Cells were maintained in growth medium as described above and additionally supplemented with 25 μg/ml ascorbic-acid-2-phosphate and 5 mM beta-glycerophosphate (hereafter, osteogenic medium). Briefly, 300 ng of total RNA was reverse transcribed using High Capacity cDNA Reverse Transcription Kit (Applied Biosystems) in a 20 μl reaction. From the resulting cDNA 1 μl was amplified using Power SYBR® Green PCR Master Mix and gene-specific primers (sequences provided in Table I) in a 7500 Fast Real-Time PCR System (Applied Biosystems) following manufacturer's recommendations. The comparison between untreated and Ag-BG treated samples was performed by normalizing to 1 the average value of untreated cells.

The capability of Ag-BG to induce cell mineralization was studied under two growth conditions; in growth medium or osteogenic medium (Figure 4). Alizarin Red Staining (ARS) was used to identify calcium-containing osteocytes in mineralized cells. To make sure that the measured calcium-containing minerals were not formed by depositions induced by Ag-BG microparticles degradation [56], acellular wells, containing only Ag-BG microparticles with medium and without hBMSC, were also taken into consideration for ARS assay. After removing the transwells, 500 μL of 40mM ARS solution in distilled water (Sigma Aldrich) was mixed with the cells for 30 min. Then, the monolayers were dissolved using 500 μL of 10% acetic acid. The red dye was measured using a spectrometer at 405 nm

and the results were recorded as optical density values (OD). The comparison between untreated and Ag-BG treated samples was performed by normalizing to a value of 100% the average of the untreated cell values.

2.4 In vitro mineralization

The formation of an apatite-like phase on the surface of the Ag-BG microparticles was evaluated after the cell mineralization test in osteogenic media. The microparticles were collected from the inserted transwells and dried at room temperature before analysis. The surface morphology and elemental composition of Ag-BG before and after cell culture were compared with SEM-EDS. Samples were prepared by spreading a thin layer of powder in carbon tape, followed by metallization in osmium gas for 15 s. Images and spectrum were collected at 15 keV. Structural differences were detected using Fourier-transformed infrared – attenuated total reflectance (FTIR-ATR; Jasco FT/IR-4600) between 400 – 2000 cm^{-1} wavenumber directly on the dried powder.

2.5 In vivo bone regeneration

All experiments were conducted under the oversight of the University of Michigan animal care and use committee and following the National Institute of Health guide for the care and use of laboratory animals (NIH Publications No. 8023, revised 1978). Twenty 6-month old mice on a C57B/L6 background were randomly assigned to four groups, each containing five mice (two females and three males). Mice were anesthetized in isoflurane and defect sites aseptically prepared. Bilateral 3 mm defects on the parietal bones of each mouse were created using a Mectron Piezosurgery drill with an OT11 osteotomy bit under saline irrigation [57]. These defects were filled with collagen sponges (Pfizer Gelfoam), sectioned to a 3 mm diameter size, loaded with a suspension of 10.5 mg Ag-BG microparticles in either 40 μl phosphate buffer solution (PBS) or natural extracellular matrix (ECM) hydrogel (from urinary bladder matrix) [58], hereafter Ag-BG/PBS and Ag-BG/ECM, respectively. As negative controls, defects were filled with collagen sponge loaded with 40 μl of ECM or PBS. The loading was performed by pipetting the slurry solution (Ag-BG/PBS, Ag-BG/ECM, PBS or ECM) into the sponge before clinical implantation. The skin was closed using 3M Vetbond surgical adhesive and, after 30 days, mice were euthanized by CO_2 asphyxiation, and tissues were collected for analysis. Skulls were scanned in a GE Healthcare eXplore Locus specimen MicroCT and analyzed in Parallax Microview using a 2.9 mm diameter x 2 mm high cylindrical region of interest centered within each defect. The formation of new bone in cranial defects was assessed by microCT analysis (1200 HU as the threshold). Following microCT, calvaria were demineralized, embedded, and cross-sectioned. The new bone area in the defect was determined using ImageJ.

2.6 Statistical analysis

All the above-mentioned *in vitro* experiments were repeated three times containing triplicates of each sample. The data was recorded as the representative mean ± one SD. The significant difference among *in vitro* sets was performed using the two-tailed Student's t-test and significance reported when $p < 0.05$. One-way ANOVA followed by the Two-stage step-up method of Benjamini, Krieger, and Yekutieli was used to analyze microCT and histology

data using GraphPad Prism 8.2.1 (GraphPad Software, San Diego, California USA, www.graphpad.com).

3 Results

3.1 Reactivation of vancomycin at different concentrations of Ag-BG against MRSA.

One of the most well-studied characteristics of Ag-BG microparticles is the antibacterial activity that was observed against several oral bacteria such as *Escherichia coli*, *Enterococcus faecalis*, *Lactobacillus casei*, and *Streptococcus mutans* [47]. The capability of Ag-BG to synergize with cell-wall targeting antibiotics, such as vancomycin, under growth-arrested conditions against MRSA was previously shown for a single combination of 0.5 mg/ml vancomycin with 2.5 mg/mL of Ag-BG [55]. Here, the concentration dependence of the synergy was studied for different combinations of Ag-BG and vancomycin to identify the minimum concentrations required to observe a synergistic antibacterial effect. The inhibition of MRSA by increasing concentration of vancomycin and Ag-BG is presented in Figure 1 a and Figure 1 b, respectively [55]. Under growth-arrested conditions, MRSA resists vancomycin, demonstrating no reduction of CFU/mL after 24 h treatment. However, MRSA is highly sensitive to Ag-BG microparticles treatment with MIC and MBC of 2.5 and 6.25 mg/mL, respectively.

To determine how the concentration of Ag-BG affects the bactericidal activity of Ag-BG/vanc, we increased the Ag-BG concentration, but exposed cells to a constant concentration of vancomycin, 0.5 mg/mL. Results revealed that increasing the concentration of Ag-BG (1.25 – 6.25 mg/mL) leads to an elevated bacteriocidal effect when MRSA was exposed to a to 0.5 mg/mL vancomycin (Figure 1 c). A combination of 0.5 mg/mL of vancomycin with 1.25 mg/mL of Ag-BG did not reduce bacterial viability to a statistically significant difference. However, increasing the concentration of Ag-BG to 2.5 mg/mL in Ag-BG/vanc inhibits MRSA CFUs to those similar to those observed when MRSA is exposed to 3.75 mg/mL of Ag-BG alone.

To determine how the concentration of vancomycin affects Ag-BG/vanc, MRSA was exposed to increasing concentrations of vancomycin, while the Ag-BG concentration remained constant at 2.5 mg/mL. These experiments revealed that elevating the concentrations of vancomycin (from 0.1 to 1 mg/mL) when combined with 2.5 mg/mL Ag-BG reduces bacterial viability and that complete sterility was achieved when 1 mg/mL of vancomycin is combined with 2.5 mg/mL of Ag-BG (Figure 1 d). Reducing the concentration of vancomycin to 0.1 mg/mL did not reduce bacterial CFUs beyond that provided by 2.5 mg/mL of Ag-BG alone. However, 0.3 mg/mL of vancomycin was identified as the minimum concentration required to observe synergy between both antibacterial agents.

3.2 Cell viability and proliferation

Experiments were done to test the viability and proliferation of hBMSC cells in a growth medium. Different concentrations of Ag-BG (2.5, 5, 7.5, and 12.5 mg) were co-cultured with cells, and proliferation was assessed by OD measurements of dissolved formazan layers.

Figure 2 a presents similar cell viability and proliferation for untreated and Ag-BG treated cells at each time point. After 2 days of co-culture cell viability is statistically lower for Ag-BG treated cells, slightly decreasing viability as the concentration of Ag-BG increases from 2.5 to 12.5 mg. However, for longer time points there is no significant difference between the treated groups and control. This result shows primary human osteoblast progenitor cells can continue to grow in the presence of increasing concentrations of Ag-BG microparticles. The proliferation rates were also observed by linear fitting the OD values of each group from day 2 to 6 (Figure 2 b) and calculating the slope of the trend for R^2>0.9. The proliferation rate of Ag-BG treated cells is double that of untreated cells. The proliferation rate did not significantly change by increasing the concentration of Ag-BG.

3.3 Cell differentiation.

Moreover, the capability of Ag-BG microparticles to induce cell differentiation was observed under both growth and osteogenic conditions. RT-PCR for the detection of gene markers was performed after 10 days of co-culture (Figure 3). Bone sialoprotein (BSP) is a significant component of the bone extracellular matrix [59] and was significantly upregulated after treatment with Ag-BG. The expression of osteocalcin (OCN) increases with bone mineral density [60]. In our experiments, it was determined that the OCN gene expression also increased after treatment with elevated concentrations of Ag-BG (7.5 and 12.5 mg).

Bone tissue is characterized by its high content of the mineral phase. The differentiation of hBMSC should be also correlated with the secretion of Ca containing minerals by the cells. The mineralization of the cells before and after Ag-BG treatment was studied via Alizarin Red Staining (ARS). It was observed that in the growth medium, the presence of Ag-BG microparticles provided a slight increase in the mineral formation compared to untreated cells (Figure 4 a–b). A higher mineral formation was detected for a higher concentration of Ag-BG treatment. Under osteogenic media, there is a notable mineral phase difference between the untreated and the Ag-BG treated cells with a 400 % increase (Figure 4 c–d). In this case, different amounts of Ag-BG did not reveal any difference among sets. Optical microscope images of the hBMSC (Figure 4 b and d) showed that after 10 days of culture, cells had almost reached confluence. Acellular wells (containing only Ag-BG with media) were also analyzed to confirm that the formation of the observed minerals is not due to depositions from the microparticles. The lack of red stain in these wells proved that the mineral phase measured in Ag-BG treated cells belonged solely to the differentiation of hBMSC.

3.4 Bioactive response by a calcium-phosphate phase formation on Ag-BG microparticles after immersion in cell culture media

The apatite-forming ability of Ag-BG microparticles has been studied in acellular *in vitro* cultures in SBF in our previous work [47]. Here, we present the deposition of an apatite-like phase at the surface of Ag-BG after 10 days of co-culture with hBMSC cells in the osteogenic medium by using SEM-EDS and FTIR. As synthesized Ag-BG microparticles present a relatively smooth surface (Figure 5 a–b) with the presence of smaller size particles on the surface of the bigger particles. After co-culture, the surface of Ag-BG microparticles

presents the formation of cauliflower deposits with a composition rich in Ca and P with Ca/P ratio close to 1.8, indicating the development of an apatite-like phase, as observed by the EDS spectrums (Figure 5 c–d).

The formation of mineral apatite in the surface of Ag-BG also modified the intensity and features of structural vibration in IR spectra (Figure 5 e). As synthesized Ag-BG presented a glass-ceramic structure with a weak presence of a calcium-phosphate phase as revealed by the double broad peak of P-O at 575 and 620 cm^{-1}. After cell exposure, the intensity of these bands increases proving the increase in the crystallinity and size of this calcium-phosphate phase at the surface as observed in Figure 5 c–d. The region at 900–1200 cm^{-1} also presents slightly different features for Ag-BG as-synthesized and after cell culture. The bands at 900 and 1200 cm^{-1} form stronger and better-defined shoulders after exposure to cells. These features are attributed to a stronger P-O bending vibration in the structure as a consequence of the apatite-like phase deposition. The nature of the deposits was further confirmed with XRD (Figure S3), where the main crystalline contributions appeared at 26° and 32°, confirming the presence of carbonated hydroxyapatite according to ICCD standards (PDF No. 9003552). These results demonstrate that the bioactive behavior of Ag-BG yielded to the well-established deposition of minerals at their surface while simultaneously triggering the secretion of minerals in the exposed cells.

3.5 Bone regenerative properties of Ag-BG in vivo

Collagen scaffolds were loaded successfully with Ag-BG microparticles as it is presented in Figure 6 a. SEM images show that the sponges were fully infiltrated by microparticles (Figure 6 a). The microCT analysis on the harvested calvarial bone tissue (Figure 6 c) showed a significantly higher fraction of newly formed bone in defects treated with Ag-BG microparticles in comparison with Ag-BG free defects. This effect is also obvious in Figure 6 b, with the Ag-BG treated defects being partially filled. However, there was a less new bone formation in the Ag-BG-free treated defects. New bone was quantified and characterized histologically. While the 2D analysis did not show statistical significance for the Ag-BG/ECM relative to the ECM alone, the Ag-BG/PBS showed 3-fold greater bone area than the PBS control. The treatments with Ag-BG microparticles show new bone formation across the entire 3 mm gap for Ag-BG/PBS (Figure 6 d and 6 e). The treatments with PBS showed only a whip of potential new bone (Figure 6 d and 6 e).

4. Discussion

In keeping with previous reports, Ag-BG microparticles demonstrated bactericidal activity against MRSA [55]. Ag-BG antibacterial activity is based on a multi-functional mechanism consisting of a simultaneous physicochemical degradation. Degradation is related to the release of ions as well as nano-sized debris in solution. The nano-sized debris penetrates the cell-wall by creating nano-pores and, subsequently, accumulating in the cytoplasm [55]. Ion release from the bioactive glass network results from its interaction with the surrounding medium and maintains neutral pH values (7.5–7.7) when Ag-BG is immersed in Tris buffer for almost up to a month [45]. Although the release of Si, P, Ca, Na, and K ions, that make up the glass structure in bioglass, has been reported to contribute to a bactericidal osmotic

effect [61,62], most ionic-based inhibition is probably caused by the presence of the nano-sized debris and the Ag^+ ions. Heavy metal ions, such as Ag^+, demonstrate potent antibacterial activity since they provide inhibition through multiple mechanisms, reducing the capability of bacteria to resist the attack [63–67]. The concentration of Ag^+ ions released from Ag-BG after 24h of immersion in an aqueous solution was previously observed to be approximately 0.4 ppm [45], which is sufficient to damage the bacterial cell envelope [55]. A similar ion release profile is expected for the concentrations used in our study, with an increase in the concentration of the released Ag^+ ions that correlates with elevating the concentration of Ag-BG. This mechanism explains the relationship between the observed reduction in bacterial CFUs and increasing the concentration of Ag-BG (Figure 1 b).

Vancomycin inhibits cell-wall synthesis in actively dividing bacterial cells, but it is inactive in growth-arrested conditions such as those tested in this work (Figure 1 a)[68,69]. Supplementing Ag-BG microparticles with increasing concentrations of vancomycin (0.3 – 1 mg/mL) resulted in a synergistic antibacterial effect that increased with elevated concentrations of vancomycin. We hypothesize that Ag-BG restores vancomycin's antibacterial activity by activating cell-wall synthesis due to the nano-tunnels created by the Ag-BG nanoproducts. We surmise that bacteria attempt to repair damage caused by the released Ag-BG nano-size debris and Ag^+ ions by cell-wall biosynthesis [55]. However, vancomycin binds to the D-Ala-D-Ala dipeptide terminus of bacterial peptidoglycans preventing the creation of new cell-wall [70,71], leading to reduced bacterial viability

The current model predicts that the first step of inhibition depends on Ag-BG degradation. The finding that Ag-BG/vanc is bactericidal only in conditions where Ag-BG concentrations are greater than or equal to its MIC (1.25 mg/mL of Ag-BG with 0.5 mg/mL vancomycin) (Figure 1 c) supports the hypothesis that Ag-BG damage to the cell wall is the first step towards the bactericidal activity. Thus, the initial damage caused by Ag-BG is the driving force for vancomycin reactivation under growth-arrested conditions. Additionally, we predict that increasing the Ag-BG concentration (2.5 – 6.25 mg/mL) while keeping vancomycin constant (0.5 mg/mL) elevated bactericidal because of the concentration of the by-products from physicochemical degradation of Ag-BG microparticles also increases (Figure 1 c).

Vancomycin concentration in the Ag-BG/vanc system is also critical for synergy. For example, a concentration of 0.1 mg/mL of vancomycin in Ag-BG/vanc was not sufficient to reduce bacterial viability beyond what was observed with 2.5 mg/ml of Ag-BG alone (Figure 1 d). We surmise that synthesis of new cell-wall is considerably low with the treatment of 2.5 mg/mL of Ag-BG alone and conclude that the amount of damage that occurs when cells are exposed to this amount of Ag-BG is not sufficient to increase vancomycin binding to D-Ala-D-Ala dipeptide at concentrations lower than 0.3 mg/mL. This result supports the notion that low quantities of D-Ala-D-Ala dipeptide require increasing the concentration of vancomycin in Ag-BG/vanc to or above 0.3 mg/mL. This finding also supports the model that Ag-BG/vanc bactericidal activity is based on the activation of cell-wall synthesis that occurs in response to Ag-BG-dependent cell wall damage, a process that is further inhibited by vancomycin. This mechanism of action is also supported using a sub-lethal concentration of vancomycin (0.5 mg/mL). In this case, increasing the concentration of Ag-BG also elevates Ag-BG/vanc synergy (Figure 1 c).

Therefore, we hypothesize that Ag-BG-dependent cell wall damage triggers additional cell-wall synthesis, increasing D-Ala-D-Ala dipeptide.

The antibacterial behavior of Ag-BG did not compromise its bioactive and biological properties when co-cultured with hBMSCs. In particular, Ag-BG was not cytotoxic at any of the tested concentrations (Figure 2 a), similarly to the behavior previously observed in cultures with pulp cells [45,72]. The release of Si, Ca, P, Na, and K ions from the bioactive glass network enhanced the rate of cell proliferation, while the concentration of the released Ag^+ ions is expected to remain constantly below the 1.6 ppm that is nontoxic to eukaryotic cells [45,73–75]. The co-cultures of hBMSCs with Ag-BG microparticles led to an increase in the proliferation rate of the cells compared to untreated cells (Figure 2 b).

Measuring the expression level of specific osteogenic markers, we observed enhanced osteogenic gene expression in hBMSCs when co-cultured with Ag-BG (Figure 3). Bone sialoprotein (BSP) is a significant component of the bone extracellular matrix [59]. Osteocalcin (OCN) is a key hormone involved in the binding of calcium to the extracellular matrix and thus, is related to bone mineral density [60]. The upregulation of the expression levels of both genes when the concentration of Ag-BG increases in the co-treatment shows the differentiation properties of the Ag-BG microparticles. BSP and OCN are non-collagenous ECM proteins that play a key role in the mineralization of bone and dentin [76]. Both of these genes appear at high levels in mature osteoblasts, but not in their immature precursors [77]. Thus, the expression of both BSP and OCN serves as an indicator of terminal osteoblastic differentiation of hBMSC.

Besides the upregulation of these biomarkers, distinct cell mineralization was identified with ARS (Figure 4). The presence of Ag-BG triggered an enhanced formation of the mineral phase within 10 days of co-treatment. Interestingly, cell mineralization occurs not only in osteogenic medium but also in growth medium without osteogenic supplements. This effect may occur due to the super-saturation of the solution that triggers cell secretion and mineral formation [78]. Because of that, under osteogenic culture conditions, the mineral content was higher than in growth conditions. This super-saturation in the culture medium is also expected to trigger the surface reactivity of Ag-BG microparticles, which is evidenced by the deposition of calcium-reach phases. The release of ions yielded to the formation of hydroxyapatite both in *in vitro* acellular test in SBF [47], as well as in the cellular test in DMEM (Figure 5 and Figure S3). The high concentration of HCO_3^- in DMEM did not favor the formation of calcite at the surface of Ag-BG, in disagreement with other works presented in the literature [79,80]. This was evidenced by the increase in intensity in P-O vibrations in FTIR, which could only be explained by an apatite-like phase deposit since calcite lacks phosphorous in its composition, as well as the identified peaks in XRD. We hypothesize that the initial presence of hydroxyapatite in the glass-ceramic structure before immersion is responsible for this phenomenon since the growth of a pre-existing phase is more energetically appealing than the formation of a new calcite phase. The formation of hydroxyapatite is also supported by its lower enthalpy of formation (−13,314 kJ/mol [81]) compared to calcite's (−1,207 kJ/mol [82]).

Ag-BG had a remarkable effect on increasing bone regeneration in this critical-sized calvarial defect. The *in vivo* regenerative properties of Ag-BG microparticles are attributed to their physicochemical and microstructural characteristics. Previous *in vivo* studies showed the capability of these microparticles to significantly induce pulp dentin regeneration [45]. This is the first time that sol-gel derived silicate-based Ag-BG microparticles have been tested for bone regeneration. The Si and Ca ions that are released from Ag-BG have the most significant role in intracellular and extracellular pathways for osteogenesis [83]. In particular, intracellular Ca ions may trigger various mitogen-activated protein kinases for cell differentiation [84]. The release of Si ions at certain concentrations has also been proven to increase cell proliferation [85]. Extracellular Ca and Si are involved in the upregulation of OCN [84,86]. Both Si and Ca synergize affecting the metabolism of osteoblastic cells [83,87]. The effect of these two ions is also evidenced in this work since increasing the concentration of Ag-BG microparticles, and consequently, the concentration of the released ions yielded to a significant upregulation of OCN and higher mineral secretion.

Additionally, the uptake process by cell phagocytosis of the nano-sized debris, that are created during the physicochemical degradation of Ag-BG microparticles is expected to contribute to the biological response. The intracellular dissolution of the nano-size debris could result in an increased Si and Ca ion content inside the cell, inducing specific signaling for their proliferation and differentiation. This effect has previously been observed after exposing mammalian cells to bioactive glass nanoparticles [88].

5. Conclusions

Ag-BG microparticles demonstrate antibacterial activity against MRSA. Our findings show that the reactivation of vancomycin in Ag-BG/vanc occurs in conditions where Ag-BG causes sufficient damage to the bacterial cell envelope. Moreover, results demonstrate that the concentration of vancomycin is also critical for observing synergy. Understanding the synergistic mechanism of action underlying the antibacterial activity of Ag-BG and vancomycin will significantly impact current therapeutic approaches employed in combating bacteria in biofilm which evade immune and therapeutic response by decreasing bacterial replication [89]. Additionally, the bioactive and regenerative properties of Ag-BG microparticles were for the first time demonstrated *in vitro* in co-culture with hBMSCs and *in vivo* in a calvarial defect model. Ag-BG not only enhanced cell proliferation rate and osteoblastic differentiation in hBMSCs but also promoted bone formation *in vivo*. These properties, combined with the unique antibacterial activity even under growth-arrested conditions, provide evidence that Ag-BG microparticles are an excellent regenerative material for the treatment of bone defects, minimizing the risk of subsequent MRSA infections.

Supplementary Material

Refer to Web version on PubMed Central for supplementary material.

Acknowledgment

Some of the materials employed in this work were provided by the Texas A&M Health Science Center College of Medicine Institute for Regenerative Medicine at Scott & White through a grant from OPIP of the NIH (grant #P40OD011050) awarded to KH. This work was also funded with the start-up funds offered to XC and NDH at Michigan State University.

9. Bibliography

[1]. Beaumont B, When Toxins Attack Nerves, (n.d.). http://www.aerotoxicsyndrombook.com/uploads/6/0/3/8/6038702/when_toxins_attack_the_nerves.pdf.

[2]. Phelps CE, Bug/Drug Resistance: Sometimes Less Is More, Med. Care 27 (n.d.) 194–203. doi:10.2307/3765142.

[3]. Rubin RJ, Harrington C. a., Poon a., Dietrich K, Greene J. a., Moiduddin a., The economic impact of Staphylococcus aureus infection in New York City hospitals., Emerg. Infect. Dis. (1999). doi:10.3201/eid0501.990102.

[4]. Antimicrobial resistance Global Report on Surveillance, (n.d.). http://apps.who.int/iris/bitstream/10665/112642/1/9789241564748_eng.pdf.

[5]. Nair SP, Meghji S, Wilson M, Reddi K, White P, Henderson B, Bacterially induced bone destruction: mechanisms and misconceptions., Infect. Immun. 64 (1996) 2371–80. [PubMed: 8698454]

[6]. Cunningham R, Cockayne A, Humphreys H, Clinical and molecular aspects of the pathogenesis of Staphylococcus aureus bone and joint infections, J. Med. Microbiol. 44 (1996) 157–164. doi:10.1099/00222615-44-3-157. [PubMed: 8636931]

[7]. Lowy FD, Staphylococcus aureus Infections, N. Engl. J. Med. 339 (1998) 520–532. doi:10.1056/NEJM199808203390806. [PubMed: 9709046]

[8]. Norden CW, Experimental Osteomyelitis. I. A Description of the Model, J. Infect. Dis. 122 (1970).

[9]. Martinez de Tejada G, Sanchez-Gomez S, Razquin-Olazaran I, Kowalski I, Kaconis Y, Heinbockel L, Andra J, Schurholz T, Hornef M, Dupont A, Garidel P, Lohner K, Gutsmann T, David SA, Brandenburg K, Bacterial Cell Wall Compounds as Promising Targets of Antimicrobial Agents I. Antimicrobial Peptides and Lipopolyamines, Curr. Drug Targets. 13 (2012) 1121–1130. doi:10.2174/138945012802002410. [PubMed: 22664072]

[10]. Barth E, Myrvik Q, Gristina WA, In vitro and in vivo comparative colonization of Sthaphylococcus aureus and Staphylococcus epidermidis on orthopaedic implant materials, (n.d.).

[11]. Murdoch DR, Roberts SA, Fowler VG, Shah MA, Taylor SL, Morris AJ, Corey GR, Infection of Orthopedic Prostheses after Staphylococcus aureus Bacteremia, Clin. Infect. Dis. 32 (2001) 647–649. doi:10.1086/318704. [PubMed: 11181131]

[12]. Chernousova S, Epple M, Silver as antibacterial agent: Ion, nanoparticle, and metal, Angew. Chemie - Int. Ed 52 (2013) 1636–1653. doi:10.1002/anie.201205923.

[13]. Lu Z, Rong K, Li J, Yang H, Chen R, Size-dependent antibacterial activities of silver nanoparticles against oral anaerobic pathogenic bacteria, J. Mater. Sci. Mater. Med. 24 (2013) 1465–1471. doi:10.1007/s10856-013-4894-5. [PubMed: 23440430]

[14]. Ruparelia JP, Chatterjee AK, Duttagupta SP, Mukherji S, Strain specificity in antimicrobial activity of silver and copper nanoparticles, Acta Biomater. 4 (2008) 707–716. doi:10.1016/j.actbio.2007.11.006. [PubMed: 18248860]

[15]. Yoon KY, Hoon Byeon J, Park JH, Hwang J, Susceptibility constants of Escherichia coli and Bacillus subtilis to silver and copper nanoparticles, Sci. Total Environ. 373 (2007) 572–575. doi:10.1016/j.scitotenv.2006.11.007. [PubMed: 17173953]

[16]. Borkow G, Gabbay J, Copper as a Biocidal Tool, Curr. Med. Chem. 12 (2005) 2163–2175. doi:10.2174/0929867054637617. [PubMed: 16101497]

[17]. Rai M, Yadav A, Gade A, Silver nanoparticles as a new generation of antimicrobials, Biotechnol. Adv. 27 (2009) 76–83. doi:10.1016/j.biotechadv.2008.09.002. [PubMed: 18854209]

[18]. Clement JL, Jarrett PS, Antibacterial Silver, Met. Based. Drugs. 1 (1994) 467–482. doi:10.1155/MBD.1994.467. [PubMed: 18476264]

[19]. Rosenman KD, Moss A, Kon S, Argyria: clinical implications of exposure to silver nitrate and silver oxide, J Occup Med. 21 (1979) 430–435. [PubMed: 469606]

[20]. Li P, Li J, Wu C, Wu Q, Li J, Synergistic antibacterial effects of β-lactam antibiotic combined with silver nanoparticles, Nanotechnology. 16 (2005) 1912–1917. doi:10.1088/0957-4484/16/9/082.

[21]. Zheng K, Lu M, Liu Y, Chen Q, Taccardi N, Norbert H, Boccaccini AR, Monodispersed lysozyme-functionalized bioactive glass nanoparticles with antibacterial and anticancer activities, Biomed. Mater. 11 (2016) 35012–35025. doi:10.1088/1748-605X/11/3/035012.

[22]. Miguez-Pacheco V, Hench LL, Boccaccini AR, Bioactive glasses beyond bone and teeth: Emerging applications in contact with soft tissues, Acta Biomater. 13 (2015) 1–15. doi:10.1016/J.ACTBIO.2014.11.004. [PubMed: 25462853]

[23]. Jones JR, Reprint of: Review of bioactive glass: From Hench to hybrids, Acta Biomater. 23 (2015) S53–S82. doi:10.1016/j.actbio.2015.07.019. [PubMed: 26235346]

[24]. Wu C, Zhou Y, Xu M, Han P, Chen L, Chang J, Xiao Y, Copper-containing mesoporous bioactive glass scaffolds with multifunctional properties of angiogenesis capacity, osteostimulation and antibacterial activity, Biomaterials. 34 (2013) 422–433. doi:10.1016/J.BIOMATERIALS.2012.09.066. [PubMed: 23083929]

[25]. Kang X, Huang S, Yang P, Ma P, Yang D, Lin J, Preparation of luminescent and mesoporous Eu 3+ /Tb 3+ doped calcium silicate microspheres as drug carriers via a template route, Dalt. Trans 40 (2011) 1873–1879. doi:10.1039/C0DT01390K.

[26]. Kaya S, Cresswell M, Boccaccini AR, Mesoporous silica-based bioactive glasses for antibiotic-free antibacterial applications, Mater. Sci. Eng. C. 83 (2018) 99–107. doi:10.1016/J.MSEC.2017.11.003.

[27]. Hench LL, Splinter RJ, Allen WC, Greenlee TK, Bonding mechanisms at the interface of ceramic prosthetic materials, J. Biomed. Mater. Res. 5 (1971) 117–141. doi:10.1002/jbm.820050611.

[28]. Hoppe A, Boccaccini AR, Biological Impact of Bioactive Glasses and Their Dissolution Products, Front. Oral Biol 17 (2015) 22–32. doi:10.1159/000381690. [PubMed: 26201273]

[29]. Xynos ID, Edgar AJ, Buttery LDK, Hench LL, Polak JM, Gene-expression profiling of human osteoblasts following treatment with the ionic products of Bioglass® 45S5 dissolution, J. Biomed. Mater. Res. 55 (2001) 151–157. doi:10.1002/1097-4636(200105)55:2<151::AID-JBM1001>3.0.CO;2-D. [PubMed: 11255166]

[30]. Xynos ID, Hukkanen MVJ, Batten JJ, Buttery LD, Hench LL, Polak JM, Bioglass ®45S5 Stimulates Osteoblast Turnover and Enhances Bone Formation In Vitro: Implications and Applications for Bone Tissue Engineering, Calcif. Tissue Int. 67 (2000) 321–329. doi:10.1007/s002230001134. [PubMed: 11000347]

[31]. Rahaman MN, Day DE, Sonny Bal B, Fu Q, Jung SB, Bonewald LF, Tomsia AP, Bioactive glass in tissue engineering, Acta Biomater (2011). doi:10.1016/j.actbio.2011.03.016.

[32]. El-Rashidy AA, Roether JA, Harhaus L, Kneser U, Boccaccini AR, Regenerating bone with bioactive glass scaffolds: A review of in vivo studies in bone defect models, Acta Biomater (2017). doi:10.1016/j.actbio.2017.08.030.

[33]. Nommeots-Nomm A, Labbaf S, Devlin A, Todd N, Geng H, Solanki AK, Tang HM, Perdika P, Pinna A, Ejeian F, Tsigkou O, Lee PD, Esfahani MHN, Mitchell CA, Jones JR, Highly degradable porous melt-derived bioactive glass foam scaffolds for bone regeneration, Acta Biomater. (2017). doi:10.1016/j.actbio.2017.04.030.

[34]. Vogel M, Voigt C, Gross UM, Müller-Mai CM, In vivo comparison of bioactive glass particles in rabbits, Biomaterials. (2001). doi:10.1016/S0142-9612(00)00191-5.

[35]. Nandi SK, Mahato A, Kundu B, Mukherjee P, Doped Bioactive Glass Materials in Bone Regeneration, in: Adv. Tech. Bone Regen, 2016. doi:10.5772/63266.

[36]. Rahmati M, Mozafari M, Selective Contribution of Bioactive Glasses to Molecular and Cellular Pathways, ACS Biomater. Sci. Eng (2020). doi:10.1021/acsbiomaterials.8b01078.

[37]. El-Rashidy AA, Waly G, Gad A, Hashem AA, Balasubramanian P, Kaya S, Boccaccini AR, Sami I, Preparation and in vitro characterization of silver-doped bioactive glass nanoparticles

fabricated using a sol-gel process and modified Stöber method, J. Non. Cryst. Solids 483 (2018) 26–36. doi:10.1016/j.jnoncrysol.2017.12.044.

[38]. Gargiulo N, Cusano AM, Causa F, Caputo D, Netti PA, Silver-containing mesoporous bioactive glass with improved antibacterial properties, J. Mater. Sci. Mater. Med. 24 (2013) 2129–2135. doi:10.1007/s10856-013-4968-4. [PubMed: 23712538]

[39]. Diba M, Boccaccini AR, Silver-containing bioactive glasses for tissue engineering applications, in: Precious Met. Biomed. Appl, 2014. doi:10.1533/9780857099051.2.177.

[40]. Mozafari M, Moztarzadeh F, Silver-doped bioactive glasses: What remains unanswered?, InterCeram Int. Ceram. Rev (2013).

[41]. Wang YY, Chatzistavrou X, Faulk D, Badylak S, Zheng L, Papagerakis S, Ge L, Liu H, Papagerakis P, Biological and bactericidal properties of Ag-doped bioactive glass in a natural extracellular matrix hydrogel with potential application in dentistry, Eur. Cells Mater 29 (2015) 342–355. doi:10.22203/eCM.v029a26.

[42]. Wren AW, Coughlan A, Hassanzadeh P, Towler MR, Silver coated bioactive glass particles for wound healing applications, J. Mater. Sci. Mater. Med. 23 (2012) 1331–1341. doi:10.1007/s10856-012-4604-8. [PubMed: 22426653]

[43]. Palza H, Escobar B, Bejarano J, Bravo D, Diaz-Dosque M, Perez J, Designing antimicrobial bioactive glass materials with embedded metal ions synthesized by the sol-gel method, Mater. Sci. Eng. C. 33 (2013) 3795–3801. doi:10.1016/j.msec.2013.05.012.

[44]. Balamurugan A, Balossier G, Laurent-Maquin D, Pina S, Rebelo AHS, Faure J, Ferreira JMF, An in vitro biological and anti-bacterial study on a sol-gel derived silver-incorporated bioglass system, Dent. Mater. 24 (2008) 1343–1351. doi:10.1016/j.dental.2008.02.015. [PubMed: 18405962]

[45]. Chatzistavrou X, Fenno JC, Faulk D, Badylak S, Kasuga T, Boccaccini AR, Papagerakis P, Fabrication and characterization of bioactive and antibacterial composites for dental applications, Acta Biomater 10 (2014) 3723–3732. doi:10.1016/j.actbio.2014.04.030. [PubMed: 24802300]

[46]. Chatzistavrou X, Paraskevopoulos KM, Salih V, Boccaccini AR, Kasuga T, Ag-Doped Sol-Gel Derived Novel Composite Materials for Dental Applications, Key Eng. Mater. 493–494 (2011) 637–642. doi:10.4028/www.scientific.net/KEM.493-494.637.

[47]. Chatzistavrou X, Velamakanni S, Direnzo K, Lefkelidou A, Fenno JC, Kasuga T, Boccaccini AR, Papagerakis P, Designing dental composites with bioactive and bactericidal properties, Mater. Sci. Eng. C. 52 (2015) 267–272. doi:10.1016/j.msec.2015.03.062.

[48]. Lee J-H, El-Fiqi A, Mandakhbayar N, Lee H-H, Kim H-W, Drug/ion co-delivery multi-functional nanocarrier to regenerate infected tissue defect, Biomaterials. 142 (2017) 62–76. doi:10.1016/J.BIOMATERIALS.2017.07.014. [PubMed: 28727999]

[49]. El-Fiqi A, Kim T-H, Kim M, Eltohamy M, Won J-E, Lee E-J, Kim H-W, Capacity of mesoporous bioactive glass nanoparticles to deliver therapeutic molecules, Nanoscale. 4 (2012) 7475. doi:10.1039/c2nr31775c. [PubMed: 23100043]

[50]. Wu C, Chang J, Multifunctional mesoporous bioactive glasses for effective delivery of therapeutic ions and drug/growth factors, J. Control. Release. 193 (2014) 282–295. doi:10.1016/J.JCONREL.2014.04.026. [PubMed: 24780264]

[51]. Hum J, Boccaccini AR, Bioactive glasses as carriers for bioactive molecules and therapeutic drugs: A review, in: J. Mater. Sci. Mater. Med, 2012. doi:10.1007/s10856-012-4580-z.

[52]. Chatzistavrou X, Esteve D, Hatzistavrou E, Kontonasaki E, Paraskevopoulos KM, Boccaccini AR, Sol-gel based fabrication of novel glass-ceramics and composites for dental applications, Mater. Sci. Eng. C. 30 (2010) 730–739. doi:10.1016/j.msec.2010.03.005.

[53]. Chatzistavrou X, Tsigkou O, Amin HD, Paraskevopoulos KM, Salih V, Boccaccini AR, Sol-gel based fabrication and characterization of new bioactive glass-ceramic composites for dental applications, J. Eur. Ceram. Soc. 32 (2012) 3051–3061. doi:10.1016/j.jeurceramsoc.2012.04.037.

[54]. Fey PD, Endres JL, Yajjala VK, Widhelm TJ, Boissy RJ, Bose JL, Bayles KW, A genetic resource for rapid and comprehensive phenotype screening of nonessential Staphylococcus aureus genes., MBio. 4 (2013) e00537–12. doi:10.1128/mBio.00537-12. [PubMed: 23404398]

[55]. Pajares-Chamorro N, Shook J, Hammer ND, Chatzistavrou X, Resurrection of antibiotics that methicillin-resistant Staphylococcus aureus resists by silver-doped bioactive glass-ceramic

microparticles, Acta Biomater 96 (2019) 537–546. doi:10.1016/J.ACTBIO.2019.07.012. [PubMed: 31302297]

[56]. Hench LL, West JK, The sol-gel process, Chem. Rev. (1990). doi:10.1021/cr00099a003.

[57]. Youngstrom DW, Senos R, Zondervan RL, Brodeur JD, Lints AR, Young DR, Mitchell TL, Moore ME, Myers MH, Tseng WJ, Loomes KM, Hankenson KD, Intraoperative delivery of the Notch ligand Jagged-1 regenerates appendicular and craniofacial bone defects, Npj Regen. Med (2017). doi:10.1038/s41536-017-0037-9.

[58]. Freytes DO, Badylak SF, Webster TJ, Geddes LA, Rundell AE, Biaxial strength of multilaminated extracellular matrix scaffolds, Biomaterials. (2004). doi:10.1016/j.biomaterials.2003.09.015.

[59]. Fisher LW, McBride OW, Termine JD, Young MF, Human bone sialoprotein. Deduced protein sequence and chromosomal localization, J. Biol. Chem. (1990).

[60]. Lee NK, Sowa H, Hinoi E, Ferron M, Ahn JD, Confavreux C, Dacquin R, Mee PJ, McKee MD, Jung DY, Zhang Z, Kim JK, Mauvais-Jarvis F, Ducy P, Karsenty G, Endocrine Regulation of Energy Metabolism by the Skeleton, Cell. (2007). doi:10.1016/j.cell.2007.05.047.

[61]. Stoor P, Söderling E, Salonen JI, Antibacterial effects of a bioactive glass paste on oral microorganisms., Acta Odontol. Scand. 56 (1998) 161–165. doi:10.1080/000163598422901. [PubMed: 9688225]

[62]. Beales N, Adaptation of Microorganisms to Cold Temperatures, Weak Acid Preservatives, Low pH, and Osmotic Stress: A Review, Compr. Rev. Food Sci. Food Saf (2004). doi:10.1111/j.1541-4337.2004.tb00057.x.

[63]. Ovington LG, The truth about silver., Ostomy. Wound. Manage. 50 (2004) 1S–10S. [PubMed: 15499162]

[64]. Reidy B, Haase A, Luch A, Dawson K, Lynch I, Mechanisms of Silver Nanoparticle Release, Transformation and Toxicity: A Critical Review of Current Knowledge and Recommendations for Future Studies and Applications, Materials (Basel). 6 (2013) 2295–2350. doi:10.3390/ma6062295. [PubMed: 28809275]

[65]. Dibrov P, Dzioba J, Gosink KK, Häse CC, Chemiosmotic mechanism of antimicrobial activity of Ag(+) in Vibrio cholerae., Antimicrob. Agents Chemother. 46 (2002) 2668–70. doi:10.1128/AAC.46.8.2668-2670.2002. [PubMed: 12121953]

[66]. Li W-R, Xie X-B, Shi Q-S, Duan S-S, Ouyang Y-S, Chen Y-B, Antibacterial effect of silver nanoparticles on Staphylococcus aureus, BioMetals. 24 (2011) 135–141. doi:10.1007/s10534-010-9381-6. [PubMed: 20938718]

[67]. Kim JS, Kuk E, Yu KN, Kim J-H, Park SJ, Lee HJ, Kim SH, Park YK, Park YH, Hwang C-Y, Kim Y-K, Lee Y-S, Jeong DH, Cho M-H, Antimicrobial effects of silver nanoparticles., Nanomedicine. 3 (2007) 95–101. doi:10.1016/j.nano.2006.12.001. [PubMed: 17379174]

[68]. Howden BP, Davies JK, Johnson PDR, Stinear TP, Grayson ML, Reduced vancomycin susceptibility in Staphylococcus aureus, including vancomycin-intermediate and heterogeneous vancomycin-intermediate strains: resistance mechanisms, laboratory detection, and clinical implications., Clin. Microbiol. Rev. 23 (2010) 99–139. doi:10.1128/CMR.00042-09. [PubMed: 20065327]

[69]. Gardete S, Tomasz A, Mechanisms of vancomycin resistance in Staphylococcus aureus, J. Clin. Invest. 124 (2014) 2836–2840. doi:10.1172/JCI68834. [PubMed: 24983424]

[70]. Zeng D, Debabov D, Hartsell TL, Cano RJ, Adams S, Schuyler JA, McMillan R, Pace JL, Approved Glycopeptide Antibacterial Drugs: Mechanism of Action and Resistance., Cold Spring Harb. Perspect. Med 6 (2016) a026989. doi:10.1101/cshperspect.a026989. [PubMed: 27663982]

[71]. Williams DH, The glycopeptide story – how to kill the deadly 'superbugs,' Nat. Prod. Rep. 13 (1996) 469–477. doi:10.1039/NP9961300469. [PubMed: 8972102]

[72]. Chatzistavrou X, Rao RR, Caldwell DJ, Peterson AW, McAlpin B, Wang Y-Y, Zheng L, Christopher Fenno J, Stegemann JP, Papagerakis P, Collagen/fibrin microbeads as a delivery system for Ag-doped bioactive glass and DPSCs for potential applications in dentistry, J. Non. Cryst. Solids. 432 (2016) 143–149. doi:10.1016/J.JNONCRYSOL.2015.03.024.

[73]. Shahverdi AR, Fakhimi A, Shahverdi HR, Minaian S, Synthesis and effect of silver nanoparticles on the antibacterial activity of different antibiotics against Staphylococcus aureus and

Escherichia coli., Nanomedicine. 3 (2007) 168–71. doi:10.1016/j.nano.2007.02.001. [PubMed: 17468052]

[74]. Cho K-H, Park J-E, Osaka T, Park S-G, The study of antimicrobial activity and preservative effects of nanosilver ingredient, Electrochim. Acta. 51 (2005) 956–960. doi:10.1016/J.ELECTACTA.2005.04.071.

[75]. Saravanapavan P, Gough JE, Jones JR, Hench LL, Antimicrobial Macroporous Gel-Glasses: Dissolution and Cytotoxicity, Key Eng. Mater. 254–256 (2004) 1087–1090. doi:10.4028/www.scientific.net/KEM.254-256.1087.

[76]. Qin C, Baba O, Butler WT, P ost-translational M odifications of SIBLING P roteins and T heir R oles in O steogenesis and D entinogenesis, Crit. Rev. Oral Biol. Med. 15 (2004) 126–136. doi:10.1177/154411130401500302. [PubMed: 15187031]

[77]. Franceschi RT, The Developmental Control of Osteoblast-Specific Gene Expression: Role of Specific Transcription Factors and the Extracellular Matrix Environment, Crit. Rev. Oral Biol. Med. 10 (1999) 40–57. doi:10.1177/10454411990100010201. [PubMed: 10759426]

[78]. Varanasi VG, Owyoung JB, Saiz E, Marshall SJ, Marshall GW, Loomer PM, The ionic products of bioactive glass particle dissolution enhance periodontal ligament fibroblast osteocalcin expression and enhance early mineralized tissue development., J. Biomed. Mater. Res. A. 98 (2011) 177–84. doi:10.1002/jbm.a.33102. [PubMed: 21548068]

[79]. Lusvardi G, Malavasi G, Menabue L, Aina V, Morterra C, Fluoride-containing bioactive glasses: Surface reactivity in simulated body fluids solutions, Acta Biomater (2009). doi:10.1016/j.actbio.2009.06.009.

[80]. Mozafari M, Banijamali S, Baino F, Kargozar S, Hill RG, Calcium carbonate: Adored and ignored in bioactivity assessment, Acta Biomater (2019). doi:10.1016/j.actbio.2019.04.039.

[81]. Flora NJ, Yoder CH, Jenkins HDB, Lattice Energies of Apatites and the Estimation of ΔH f° (PO43-,g), Inorg. Chem. (2004). doi:10.1021/ic030255o.

[82]. Zumdahl S, Decoste D, Chemical Principles, 8th Ed. TEXTBOOK, 2006. doi:10.1002/0471743984.vse5459.pub2.

[83]. Dufrane D, Delloye C, McKay IJ, De Aza PN, De Aza S, Schneider YJ, Anseau M, Indirect cytotoxicity evaluation of pseudowollastonite, J. Mater. Sci. Mater. Med. 14 (2003) 33–38. doi:10.1023/A:1021545302732. [PubMed: 15348536]

[84]. Maeno S, Niki Y, Matsumoto H, Morioka H, Yatabe T, Funayama A, Toyama Y, Taguchi T, Tanaka J, The effect of calcium ion concentration on osteoblast viability, proliferation and differentiation in monolayer and 3D culture, Biomaterials. 26 (2005) 4847–4855. doi:10.1016/J.BIOMATERIALS.2005.01.006. [PubMed: 15763264]

[85]. Valerio P, Pereira MM, Goes AM, Leite MF, The effect of ionic products from bioactive glass dissolution on osteoblast proliferation and collagen production, Biomaterials. 25 (2004) 2941–2948. doi:10.1016/J.BIOMATERIALS.2003.09.086. [PubMed: 14967526]

[86]. Reffitt D, Ogston N, Jugdaohsingh R, Cheung HF, Evans BA, Thompson RP, Powell J, Hampson G, Orthosilicic acid stimulates collagen type 1 synthesis and osteoblastic differentiation in human osteoblast-like cells in vitro, Bone. 32 (2003) 127–135. doi:10.1016/S8756-3282(02)00950-X. [PubMed: 12633784]

[87]. Saffarian Tousi N, Velten MF, Bishop TJ, Leong KK, Barkhordar NS, Marshall GW, Loomer PM, Aswath PB, Varanasi VG, Combinatorial effect of Si4 +, Ca2 +, and Mg2 + released from bioactive glasses on osteoblast osteocalcin expression and biomineralization, Mater. Sci. Eng. C. 33 (2013) 2757–2765. doi:10.1016/J.MSEC.2013.02.044.

[88]. Naruphontjirakul P, Tsigkou O, Li S, Porter AE, Jones JR, Human mesenchymal stem cells differentiate into an osteogenic lineage in presence of strontium containing bioactive glass nanoparticles, Acta Biomater. 90 (2019) 373–392. doi:10.1016/j.actbio.2019.03.038. [PubMed: 30910622]

[89]. Esposito S, Leone S, Prosthetic joint infections: microbiology, diagnosis, management and prevention, Int. J. Antimicrob. Agents. (2008). doi:10.1016/j.ijantimicag.2008.03.010.

Highlights

- Ag-BG is antibacterial against MRSA in a biofilm-simulated environment.
- Ag-BG synergizes with vancomycin, inhibiting significantly planktonic MRSA at very low concentrations of the two agents. The critical concentrations were identified for optimum combinatorial therapy.
- Ag-BG enhances cell proliferation and differentiation.
- Ag-BG induces bone regeneration in *in vivo* mouse calvarial model.

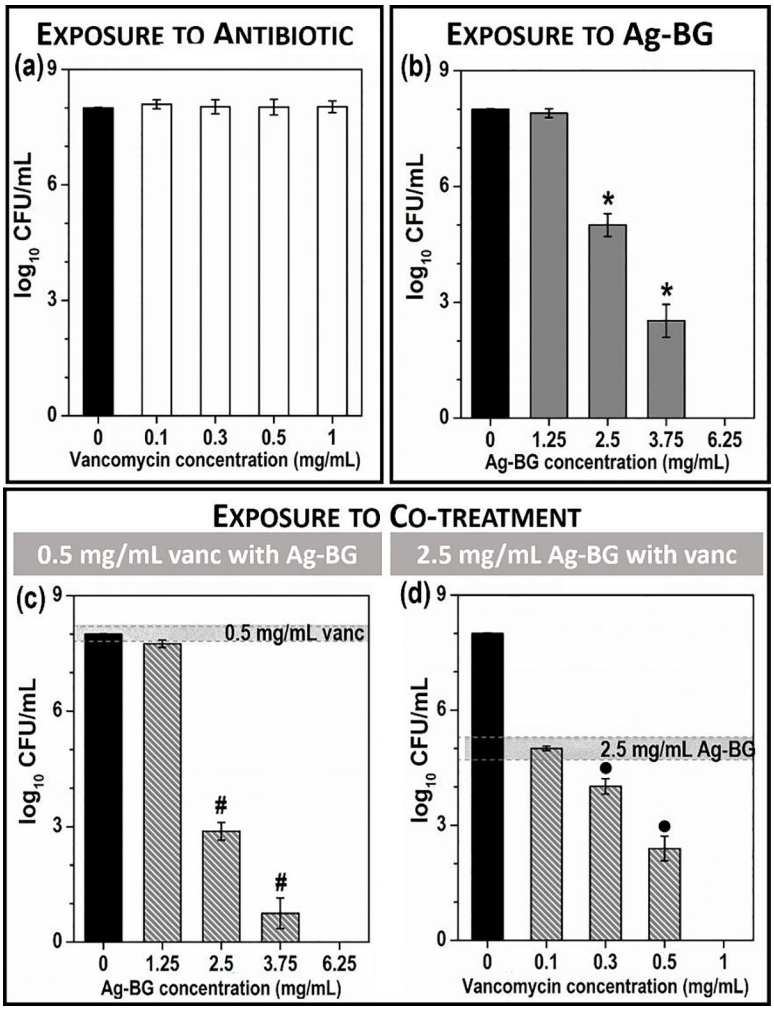

Figure 1:

Ag-BG synergizes with vancomycin against MRSA in PBS. The minimum inhibitory concentration of vancomycin (a) and Ag-BG (b), reproduced from [55]. Statistical significance ($p<0.05$) between Ag-BG and untreated marked with (*). (c) MRSA exposed to 0.5 mg/mL vancomycin with increasing concentration of Ag-BG, where (#) indicates statistical significance ($p<0.05$) between 0.5 mg/mL of vancomycin and Ag-BG/vanc. (d) MRSA exposed to 2.5 mg/mL Ag-BG with increasing concentration of vancomycin where (•) indicates statistical significance between 2.5 mg/mL of Ag-BG and Ag-BG/vanc.

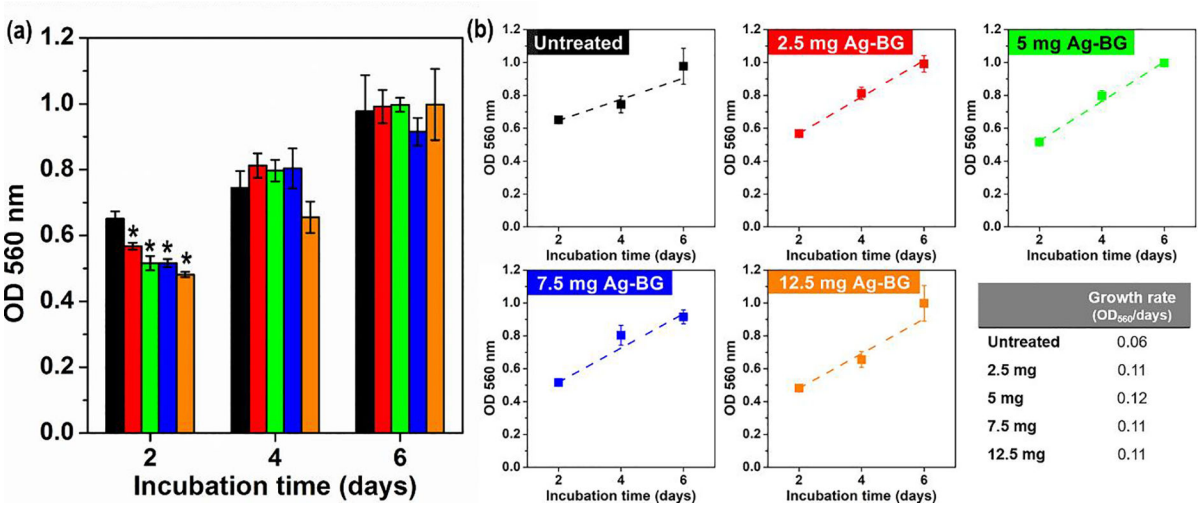

Figure 2:

Proliferation rate of hBMSC cells when co-cultured with different concentrations of Ag-BG. The significant difference ($p < 0.05$) between untreated and Ag-BG treated cells is indicated with (*).

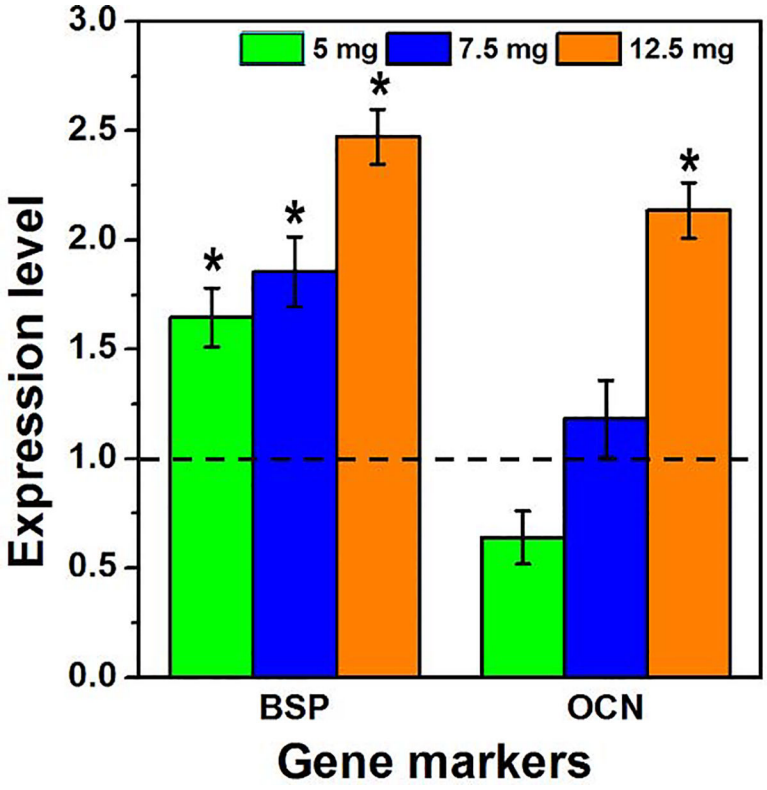

Figure 3:

Expression level for bone sialoprotein (BSP) and osteocalcin (OCN) gene markers after 10 days in osteogenic media with 5, 7.5, and 12.5 mg of Ag-BG. Gene expression level of untreated cells was normalized to 1 (dashed line). The significant difference ($p < 0.05$) between untreated and Ag-BG treated cells is indicated with (*).

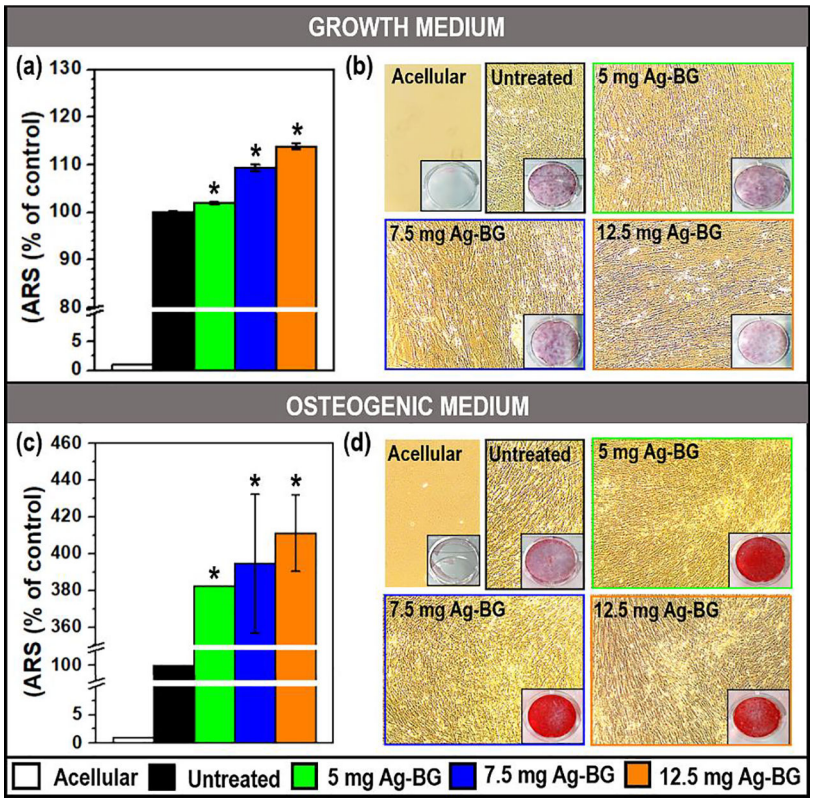

Figure 4:

hBMSC differentiation with Alizarin Red Staining (ARS) in growth (a-b) and osteogenic medium (c-d). Optical density (a and c) was normalized utilizing untreated cells as 100 %. Fibroblast optical images (b and d) with ARS wells as inserts. (*) Statistical difference between untreated and Ag-BG treated cell for $p<0.05$.

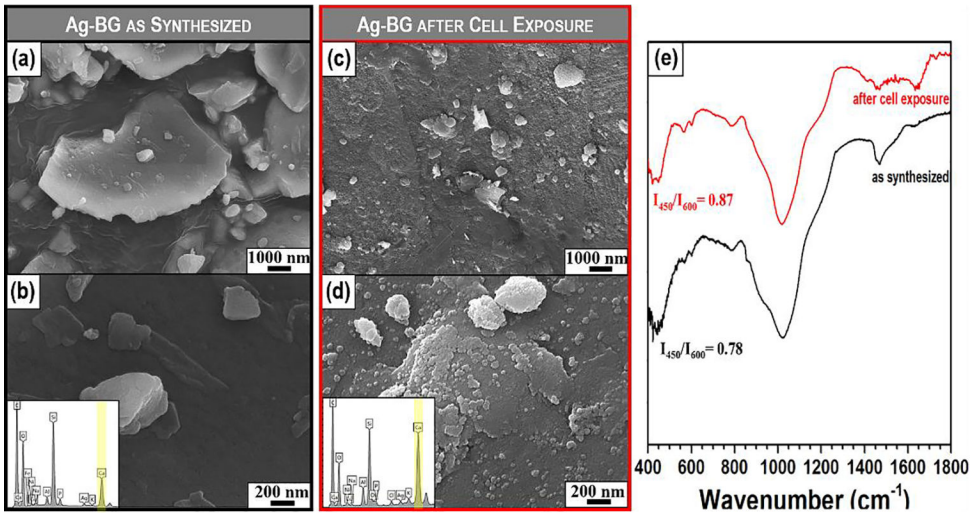

Figure 5:

Apatite forming ability of Ag-BG. The surface of the microparticles as-synthesized and after 10 days in cell culture (a-d). EDS spectrum of Ag-BG surface as-synthesized and after cell-culture appear as inserts in b and d, respectively. FTIR spectra of Ag-BG microparticles before (black line) and after (red line) exposure to cells (e).

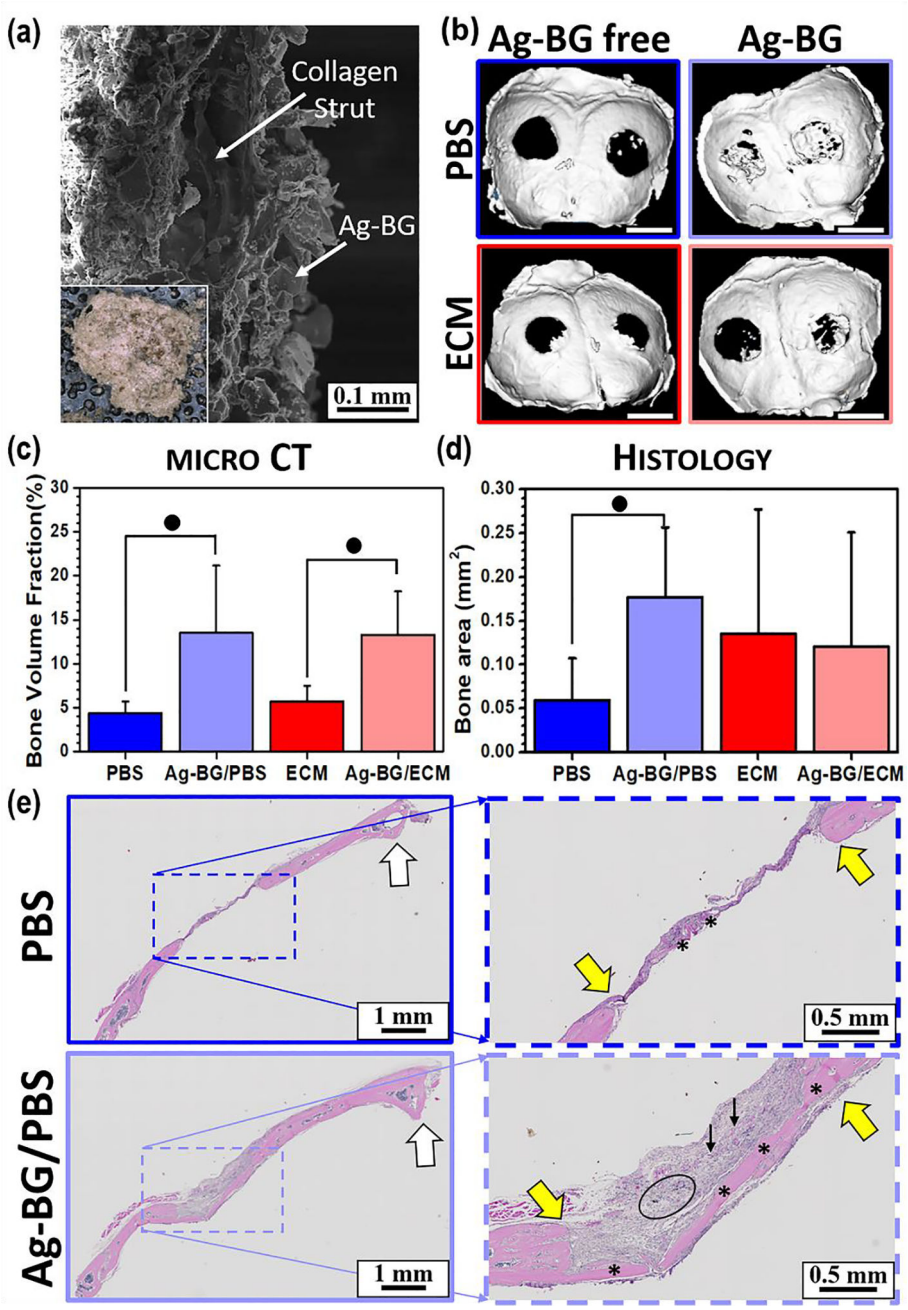

Figure 6:

SEM image from the cross-section of a representative collagen sponge loaded with Ag-BG microparticles (a) where inset shows the optical top view of the implant. Representative microCT images of the calvaria, where white scale bar represents 3 mm (b). Bone volume fraction of the new bone formed (c), and 2D assessment of bone area (d) in the defect area under different treatments for n=5 animals with 2 defects/animal. ● identifies statistical significance $p<0.05$ between marked groups. Coronal cross-sections of calvaria are divided in half along the sagittal crest (e) where * indicates the presence of significant soft-tissue as well as bone. Edges of the defect are indicated by yellow arrows, the circle indicates retained

Ag-BG, and black arrows point to collage sponge. Note that PBS treated defect shows little overall regenerative response.

Table I:

List of Primer used for qRT-PCR analyses

Primer Name	Sequence (5'–3')
hGAPDH_S	TGGTATCGTGGAAGGACTCATGAC
hGAPDH_AS	ATGCCAGTGAGCTTCCCGTTCAGC
hBSP_S	ACAACACTGGGCTATGGAGA
hBSP_AS	CCTTGTTCGTTTTCATCCAC
hOCN_S	CACCGAGACACCATGAGAGC
hOCN_AS	CGGATTGAGCTCACACACCT